Supplementary Information

A cell-based screen identifies ATR inhibitors with synthetic lethal properties for cancer-associated mutations

Luis I. Toledo[1], Matilde Murga[1], Rafal Zur[1], Rebeca Soria[1], Antonio Rodriguez[2], Sonia Martinez[2], Julen Oyarzabal[2,3], Joaquin Pastor[2], James R. Bischoff[2] & Oscar Fernandez-Capetillo[1]

[1]Genomic Instability Group, Spanish National Cancer Research Centre (CNIO), Madrid, Spain. [2]Experimental Therapeutics Programme, Spanish National Cancer Research Centre (CNIO), Madrid, Spain. [3]Present address: Center for Applied Medical Research (CIMA), University of Navarra, Pamplona, Spain. Correspondence should be addressed to O.F. (ofernandez@cnio.es)

a

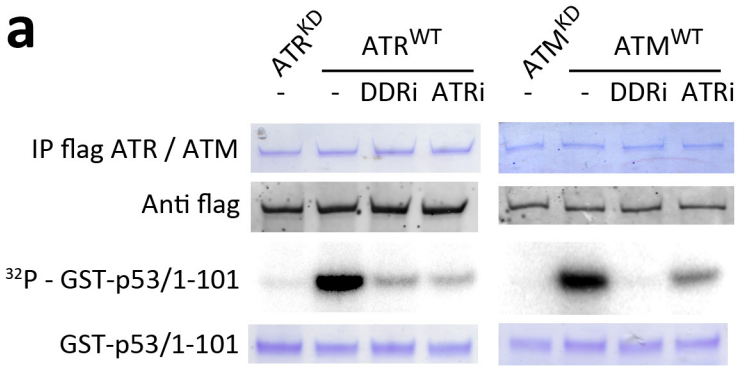

b

Protein Kinase	ATRi (5 μM)		DDRi (10 μM)	
	% Inhibition			
Akt 1	0	1	13	9
Ark5	13	9	7	18
B-Raf (V600E)	12	54	19	22
Cdk8/Cyc C	ND	ND	13	25
CK1-alpha1	11	11	2	12
DYRK 1A	15	7	25	8
EGF-R	14	13	58	60
ERK1	55	0	ND	ND
FAK	20	20	57	59
FGF-R1	23	16	61	40
FLT3	16	0	67	64
IGF-R1	21	20	75	71
IKK-beta	8	23	0	0
INS-R	ND	ND	46	50
JAK2	12	7	79	56
JNK1	ND	ND	41	38
MEK1	7	13	2	0
MET	6	14	47	45
MST1	11	16	54	47
PAK1	0	20	7	3
p38-alpha	0	0	ND	ND
PDGFR-alpha	0	7	48	45
PIM1	9	22	32	4
PIM2	8	4	6	23
RPS6KA1	31	10	0	36
SGK1	0	1	5	16

c

Kinase	ATRi IC_{50} (nM)	DDRi IC_{50} (nM)
PI3Kα	170	2
mTOR	0.6	2
DNA PK	36	5
ATM	545	7
ATR	14	21

Supplementary Figure 1 *In vitro* activity of the ATR inhibitors**. a,** *In vitro* kinase assays of flag-ATM and flag-ATR (wild type [WT] and kinase dead [KD] versions) immunoprecipitated (IP) from 293T cells were performed with a substrate harbouring the first 101 aminoacids of p53 (GST-p53/1-101) (see Methods). The example illustrates that: (a) both compounds are capable of inhibiting the kinase activities *in vitro* and, (b) that the ATRi is still significantly selective towards ATR *vs* ATM even at high doses (10 μM) of the compounds. **b,** Effect of ATRi and DDRi against a panel of 26 protein kinases. Two independent assays were performed at the concentrations indicated. The percent inhibition relative to DMSO control is given. Assays were performed at ProQinase GMBH. **c,** *In vitro* IC_{50} of the ATRi and DDRi for ATM, ATR, PI3Ka, mTOR and DNA PK. Assays for calculating the IC_{50} of PI3Ka, mTOR and DNA PK were performed with recombinant kinases as described in Link et al[1]. In contrast, the IC_{50} for ATM and ATR were calculated using flag-IP assays as the one illustrated in **a.**

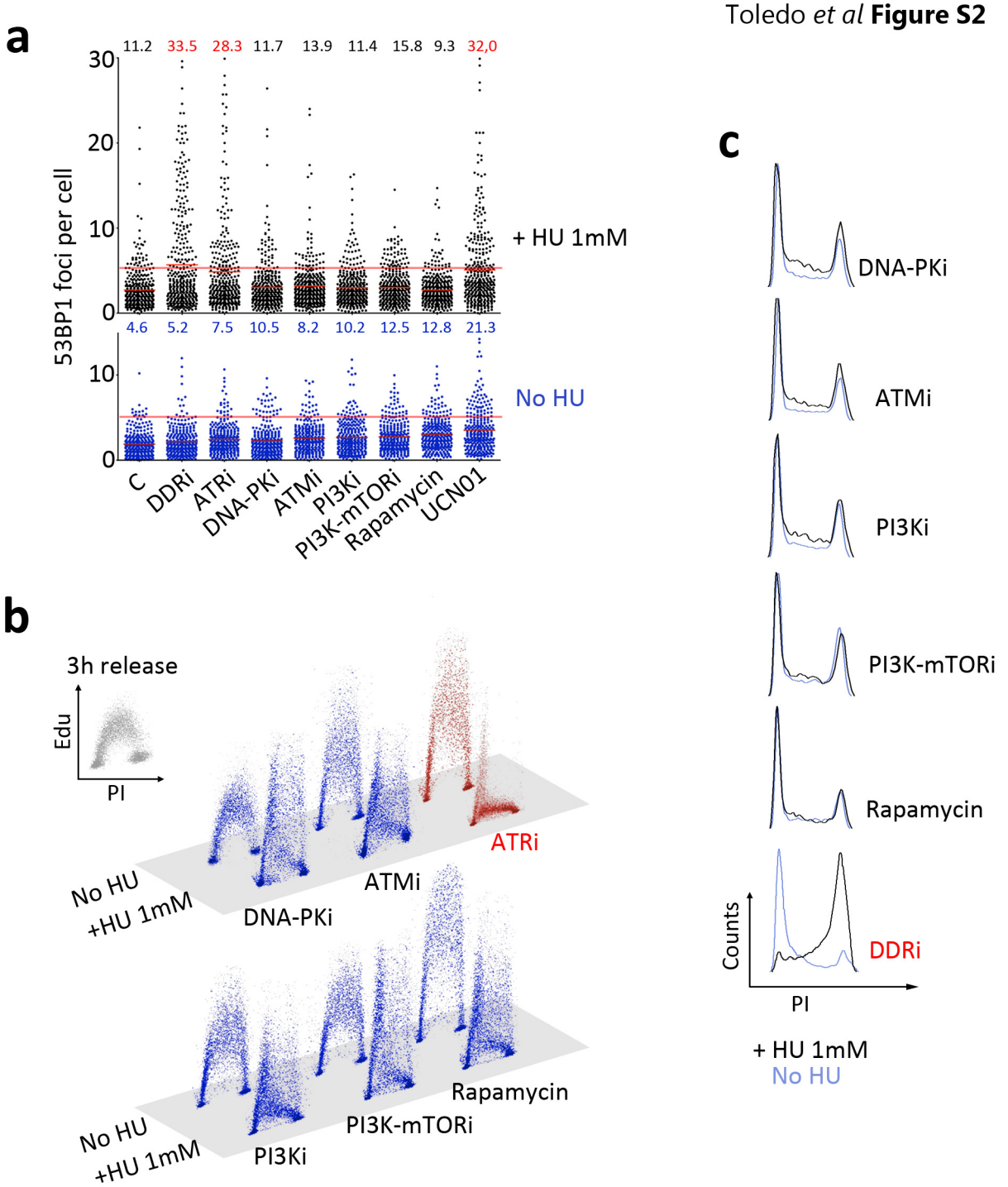

Supplementary Figure 2 The role of the inhibitors in stabilizing stalled replication forks is independent of ATM, DNA-PK, PI3K and mTOR**. a,** Breakage of stalled replication forks. The figure illustrates the number of 53BP1 foci induced by a 3 hr HU treatment in the presence of the different inhibitors as quantified by HTM. Note that only ATRi, DDRi and UCN-01 lead to significant breakage after HU. **b,** Restart of stalled replication forks was quantified by a pulse of EdU (1hr), performed 3 hrs after the release from a 3hr exposure to HU (1mM). **c**, G2-induced arrest in response to HU. Cells were exposed to HU for 3hrs in the presence of the indicated inhibitors, and then released into free media for another 16 hrs. The G2-arrest was strictly dependent on ATR and did not occur with any of the other inhibitors.

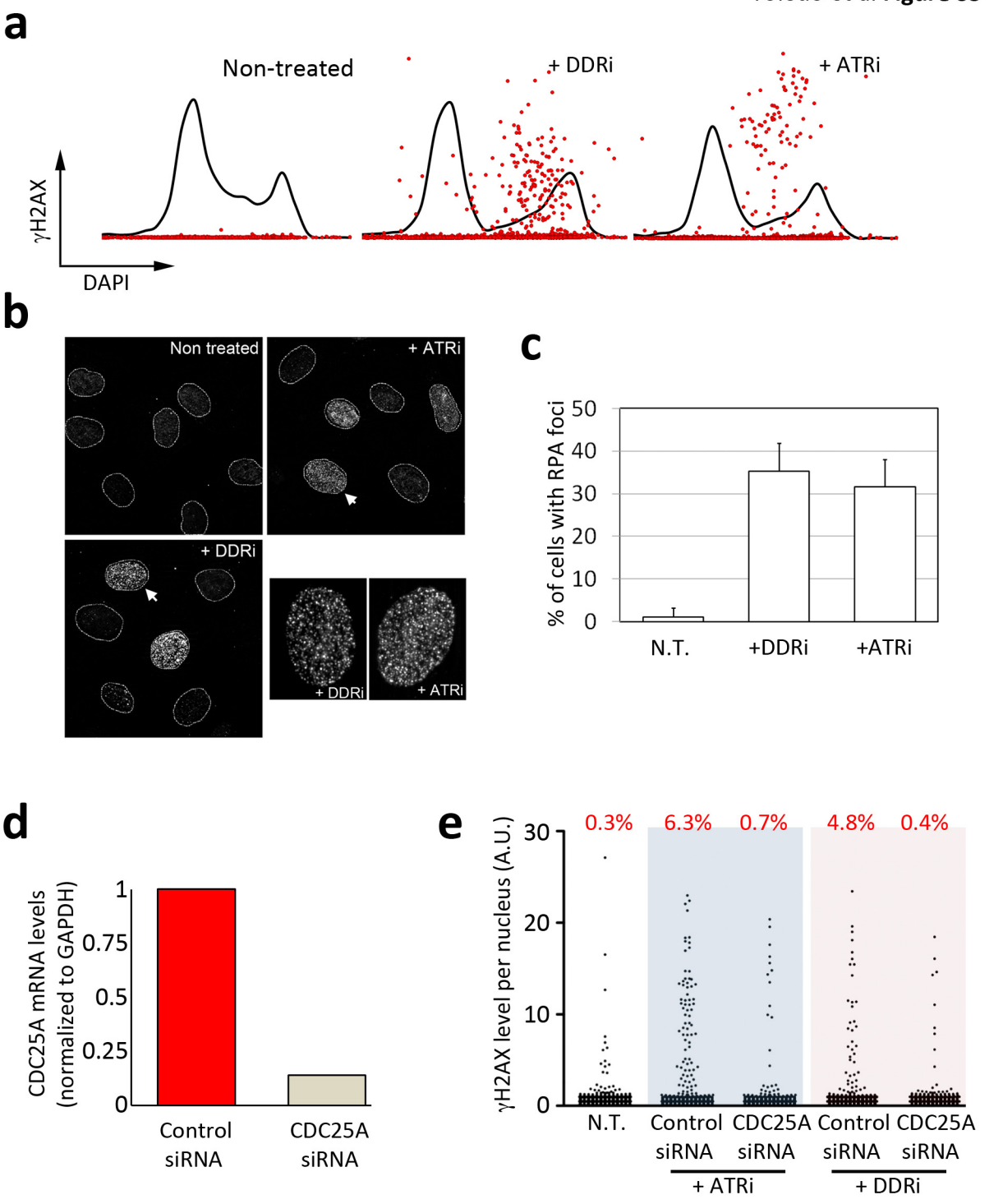

Supplementary Figure 3 ATR inhibitors promote the generation of RS. **a,** HTM data from U2OS cells exposed to the inhibitors for 4 hrs was represented against the DAPI signal [ATRi and DDRi: 5 μM]. **b,** Distribution of RPA in U2OS cells treated as in **a**. **c,** Quantification of the number of cells presenting a uniform distribution of bright RPA foci as shown in **b**. Note that the frequency is similar to the fraction of replicating cells. **d,** Efficiency of the RNAi-mediated knockdown of CDC25A in U2OS quantified by qRT-PCR. **e,** The generation of RS was quantified by HTM by analyzing the levels of nuclear γH2AX in U2OS that had been previously transfected for 48 hrs with CDC25A-targeting or Control siRNAs, and exposed to the ATR inhibitors as shown in **a**. For the CDC25A targeting siRNAs, we use the same sequence that was published to work in decreasing the load of S-phase DNA damage induced by Chk1 inhibitors[2].

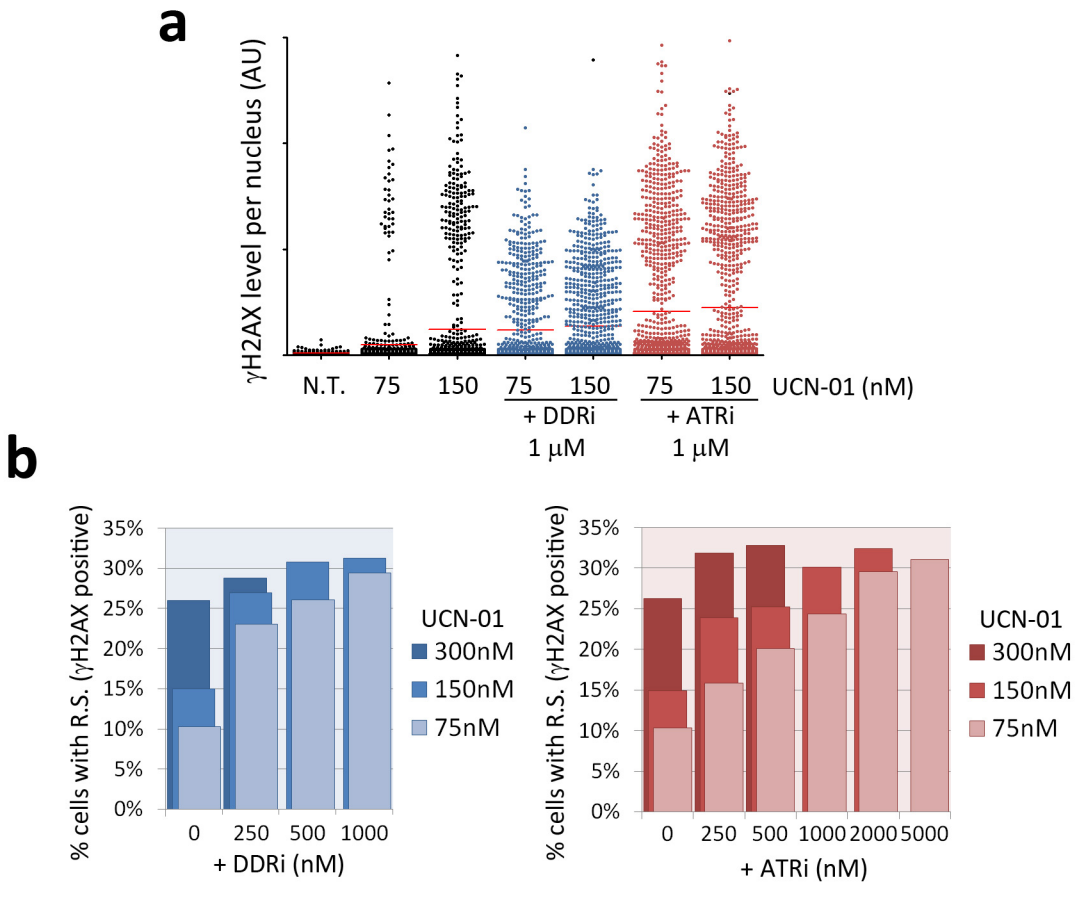

Supplementary Figure 4 Dual inhibition of ATR and Chk1 increases RS in a cooperative fashion. **a**, The levels of RS generated by a low dose of UCN-01 are enhanced in combination with DDRi or ATRi (note that these concentrations of the inhibitors do not generate RS by themselves). **b**, Quantification of the % of cells showing a pan-nuclear γH2AX staining upon a combined treatment of UCN-01 and DDRi/ATRi at growing concentrations. Note that a maximum of around 30% cells with RS is reached at the highest doses, probably reflecting the % of replicating cells during the treatment period.

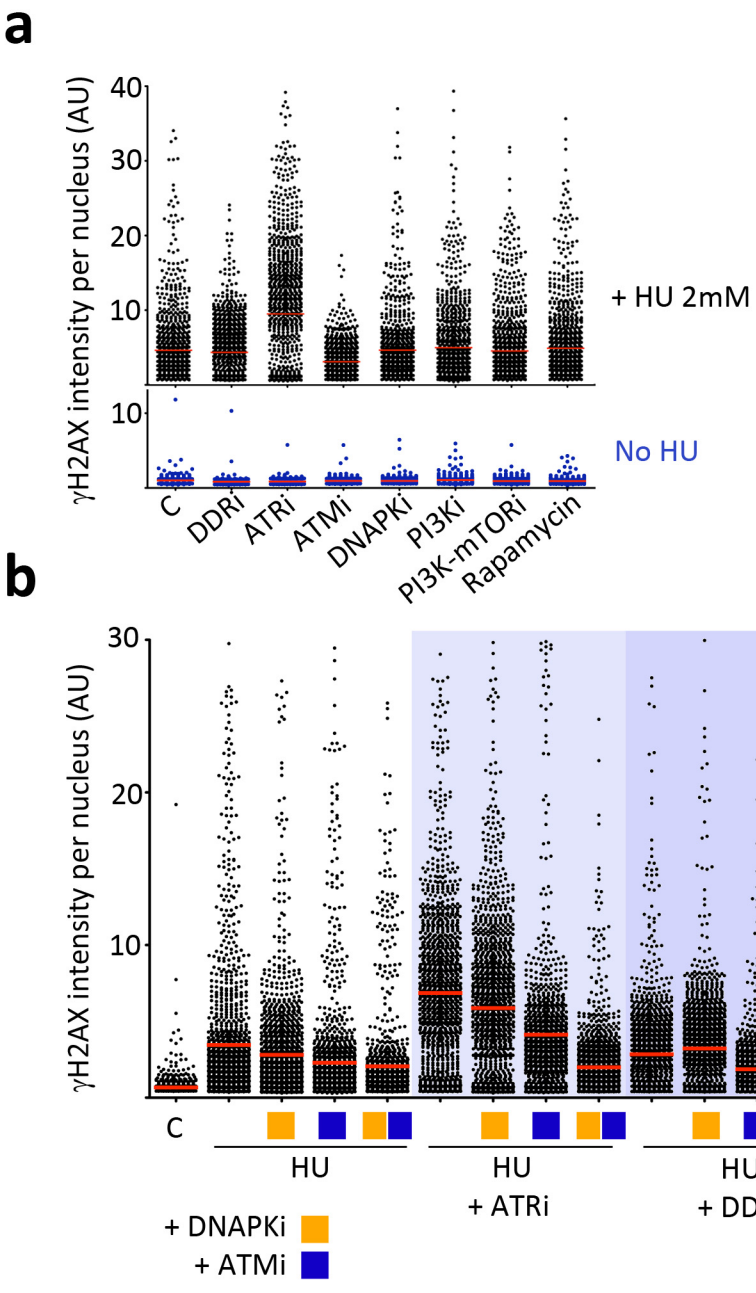

Supplementary Figure 5 The effect of the compounds in generating RS is independent of ATM, DNA-PK, PI3K and mTOR. **a,** The generation of RS was quantified by HTM by analyzing the levels of nuclear γH2AX in the presence or absence of HU and the indicated inhibitors. Note that ATM and DNA-PKcs inhibition not only do not generate cells with a pan-nuclear γH2AX staining pattern but, as previously shown, they are responsible for this phosphorylation[3].

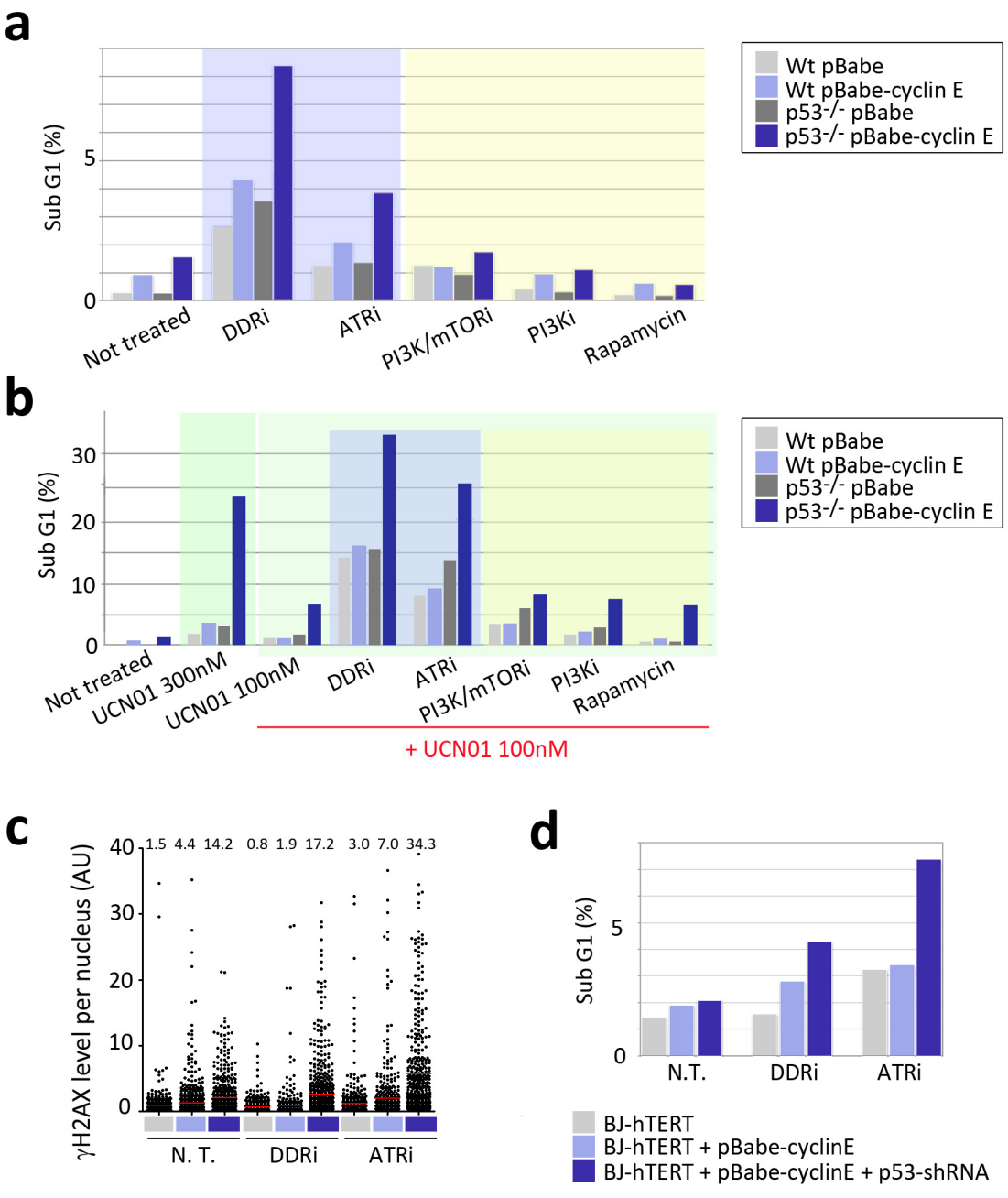

Supplementary Figure 6 The synthetic lethal effect of ATR inhibitors with cyclin E and/or p53 loss is unrelated to PI3K or mTOR. Given that the DDRi (NVP-BEZ235) is now widely being tested for cancer treatments on the basis of being a dual PI3K/mTOR inhibitor[4], it was particularly relevant that we assessed the role of PI3K and mTOR in the synthetic lethal effect with cyclin E and p53-loss. **a,** The figure illustrates that whereas ATR inhibitors are preferentially toxic for cyclin E overexpressing p53 deficient MEF the use of PI3K, mTOR or even dual PI3K/mTOR inhibitors does not display any selective toxicity for these cells (not even when combined with Chk1 inhibitors, as shown in **b**). This synthetic lethal effect of the ATR inhibitors was also observed in human cells as illustrated in **c,d. c,** HTM-mediated quantification of the nuclear γH2AX signal in telomerized human foreskin fibroblasts (BJ-hTERT) in the presence of ATRi or DDRi, upon overexpression of cyclin E, and with or without shRNA-mediated depletion of p53. **d,** Percentages of subG1 cells from BJ-hTERT cells treated as in **c**, are shown after a 48 hr treatment with the inhibitors. [ATRi and DDRi: 5 μM].

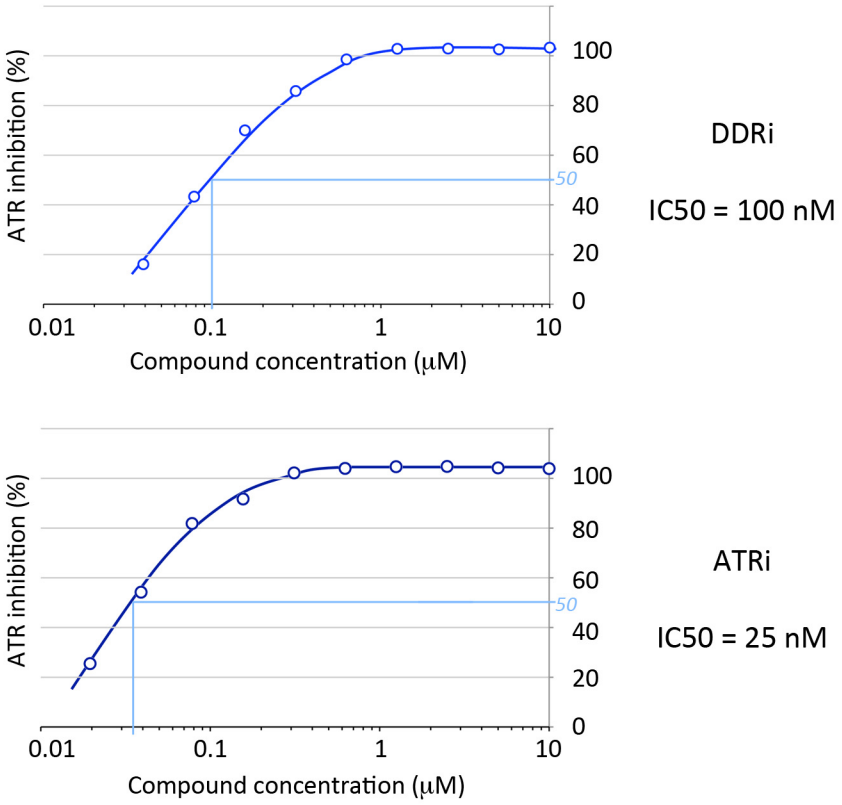

Supplementary Figure 7 IC_{50} measurements of ATRi and DDRi. **a,** The IC_{50} for ATRi and DDRi in ATR inhibition was calculated using the ATR-specific cell based assay described in **Figure 1**. Each datapoint represents the average nuclear γH2AX intensity at each indicated dose of the inhibitors. It should be noted that all these IC_{50}s where calculated *in cellulo*. Noteworthy, the *in vitro* IC_{50}s are significantly lower than the ones in cells (see discussion). For instance, whereas in cells the ATM inhibitor KU5593 is normally used in the micromolar range, the *in vitro* IC_{50} was estimated in 12.9 nM[5].

Supplementary Figure 8 Synthesis of the ATRi. The figure provides the synthesis scheme and experimental procedure used to synthesize the compound here described as ATRi.

Synthesis Scheme:

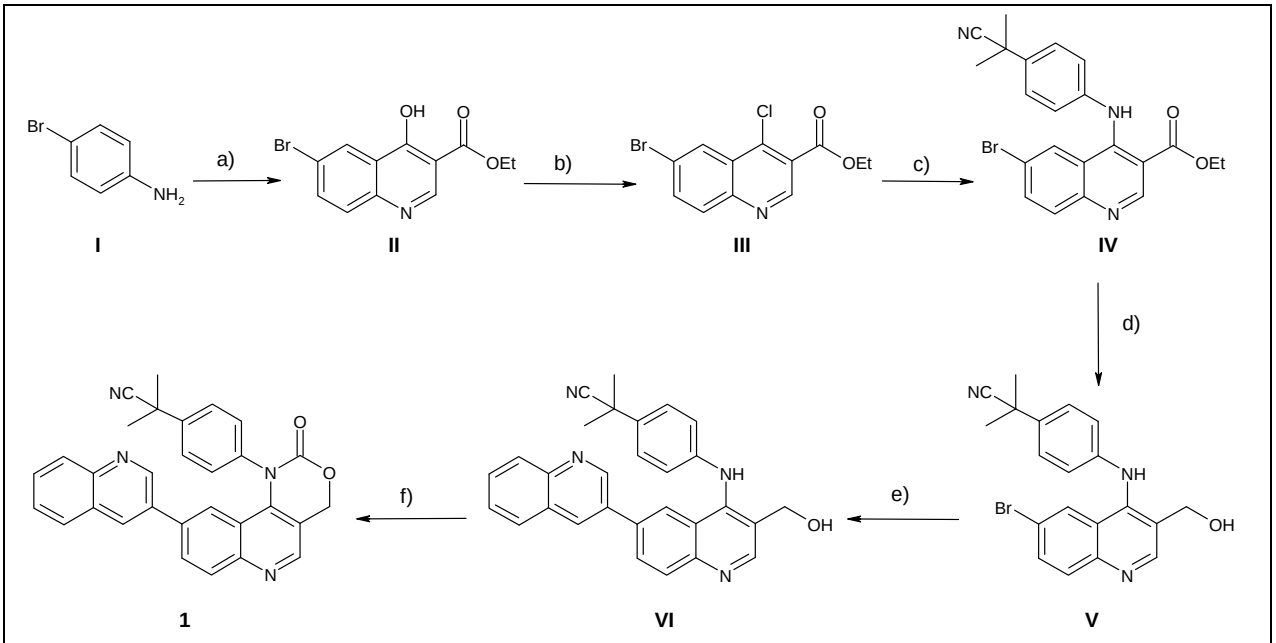

a) diethyl ethoxymethylenemalonate, 100ºC, 4h. b) $POCl_3$, 18h, reflux. c) 2-(4-Aminophenyl)-2-methylpropionitrile, AcOH, 16h, rt.
d) $LiAl(O^tBu)_3H$, THF, reflux. e) quinoline 3-boronic acid, $Pd(AcO)_2$, dppf, K_2CO_3, H_2O, DMF, 70ºC 4h. f) triphosgene, TEA, dioxane, 6h, rt

Scheme 1

Experimental Procedure

Ethyl 6-bromo-4-hydroxyquinoline-3-carboxylate (II)

4-Bromoaniline(10 g, 58.13 mmol) and diethyl ethoxymethylenemalonate (12.5g, 58.13 mmol) were mixed and stirred until homogeneous solution, then the reaction was heated at 100ºC for 4 h. Diphenyl ether was added and the mixture was heated at 280ºC for 4 h. On cooling, cyclohexane was added (~100 mL) and the resulting solid was filtered, washed (cyclohexane) and dried to give compound **II** as a brown solid (15.31 g, 89% yield).

^{1}H NMR (DMSO, 300 MHz): δ 12.45 (s, 1H, OH), 8.59 (s, 1H, 2-H), 8.22 (d, J = 2.4, 1H, 5-H), 7.87 (dd, J = 8.8, 2.4, 1H, 7-H), 7.60 (d, J = 8.8, 1H, 8-H), 4.22 (q, J = 7.1, 2H, OCH_2), 1.28 (t, J = 7.1, 3H, CH_3).

Ethyl 6-bromo-4-chloroquinoline-3-carboxylate (III)

Compound **II** (2.5 g, 8.44 mmol) was dissolved in $POCl_3$ (23.6 mL) and the mixture was refluxed for 18 h. On cooling, $POCl_3$ was removed in vacuo and the residue was suspended in water and the suspension was cooled to 0ºC. Aqueous NH_4OH was added dropwise at 0ºC up to pH~8. The resulting solid was filtered, washed with water and dried to give compound **III** as a brown solid (2.09 g, 79% yield).

^{1}H NMR (300 MHz, $CDCl_3$) δ 9.20 (s, 1H, 2-H), 8.58 (d, J = 2.1, 1H, 5-H), 8.02 (d, J = 8.9, 1H, 8-H), 7.92 (dd, J = 8.9, 2.1, 1H, 7-H), 4.52 (q, J = 7.1, 2H, OCH_2), 1.47 (t, J = 7.1, 3H, CH_3).

Ethyl 4-(4-(2-cyanopropan-2-yl)phenylamino)-6-bromoquinoline-3-carboxylate (IV)

A mixture of compound **III** (930 mg, 2.96 mmol, 1 eq) and 2-(4-Aminophenyl)-2-methylpropionitrile (521 mg, 3.25 mmol, 1.1 eq, cas: 115279-57-7) in AcOH (10 mL) was stirred overnight at room temperature. Then, the solvent was removed in vacuo and the

residue was suspended in water (15 mL). Aqueous 32% NH_4OH was added up to pH ~8 and the resulting solid was filtered off, washed with water and dried to give compound **IV** after purification by column chromatography (Hexane/EtOAc mixtures as eluent) (1.17 g, 89% yield).

^{1}H NMR (300 MHz, DMSO) δ = 9.69 (s, 1H), 8.90 (s, 1H), 8.43 (s, 1H), 7.86 (m, 2H), 7.45 (d, *J*=8.5, 2H), 7.11 (d, *J*=8.5, 2H), 3.86 (q, *J*=7.1, 2H), 1.68 (s, 6H), 1.04 (t, *J*=7.1, 3H).

Ethyl 4-(4-(2-cyanopropan-2-yl)phenylamino)-6-bromoquinoline-3-yl methanol (V)

Compound **IV** (1.15 g, 2.624 mmol, 1 eq) was added portionwise to a solution of lithium tri-tert-butoxyaluminum hydride (3.336 g, 11.12 mmol, 5 eq) in THF (50 mL) cooled to 0ºC: The mixture was refluxed for 2 days, cooled to 0ºC and quenched with MeOH (5 mL). Water (30 mL) was added and the mixture was extracted with EtOAc (4 x 250 mL).The combined organic fractions were dried (Na_2SO_4) and the solvent removed in vacuo to give a yellow residue that was purified by column chromatography (EtOAc and EtOAc/MeOH mixtures) to give compound **V** as a white solid (758 mg, 73% yield).

^{1}H NMR (300 MHz, DMSO) δ 9.00 (s, 1H, 2-H), 8.58 (s, 1H, NH), 8.22 (d, J = 2.1, 1H, 5-H), 7.95 (d, J = 8.9, 1H, 8-H), 7.83 (dd, J = 8.9, 2.2, 1H, 7-H), 7.33 (d, J = 8.7, 2H, 3-Ar), 6.72 (d, J = 8.7, 2H, 2-Ar), 5.38 (t, J = 5.4, 1H, OH), 4.44 (d, J = 5.3, 2H, CH_2O), 1.64 (s, 6H, CH_3).

2-(4-(3-methanol-6-(quinolin-3-yl)quinolin-4-ylamino)phenyl)-2-methylpropanenitrile (VI)

A mixture of compound **V** (750 mg, 1.89 mmol, 1 eq), quinoline 3-boronic acid (818 mg, 4.73 mmol, 2.5 eq), $Pd(OAc)_2$ (42 mg, 0.189 mmol, 0.1 eq), dppf (214 mg, 0.379 mmol, 0.2 eq), K_2CO_3 (1046 mg, 7.57 mmol, 4 eq) and water (7 mL) in degassed DMF (70 mL) was heated at 70ºC for 4 h under nitrogen. On cooling, the solvent was removed in vacuo

and the brown residue was purified by flash chromatography using EtOAc and EtOAc/MeOH mixtures as eluents to give compound **VI** as a brown solid (727 mg, 86% yield).

^{1}H NMR (300 MHz, DMSO) δ 9.18 (d, J = 2.3, 1H), 8.92 (s, 1H), 8.64 (s, 1H), 8.61 (d, J = 2.2, 1H), 8.42 (d, J = 1.8, 1H), 8.17 (dd, J = 8.8, 2.0, 1H), 8.09 (d, J = 8.8, 1H), 7.99 (d, J = 8.4, 2H), 7.72 (ddd, J = 8.3, 6.9, 1.4, 1H), 7.59 (ddd, J =8.0, 6.9, 1.3, 1H), 7.31 (d, J = 8.6, 2H), 6.77 (d, J = 8.7, 2H), 5.32 (t, J = 5.4, 1H), 4.42 (d, J = 5.3, 2H), 1.59 (s, 6H).

2-methyl-2-(4-(2-oxo-9-(quinolin-3-yl)-2H-[1,3]oxazino[5,4-c]quinolin-1(4H)-yl)phenyl)propanenitrile (1)

A mixture of compound **VI** (57 mg, 0.128 mmol, 1 eq) and triethylamine (0.04 ml, 0.256 mmol, 2 eq) in dioxane (1 mL) was cooled to 0ºC. Then, triphosgene (42 mg, 0.141 mmol, 1.1 eq) was added and the mixture was stirred for 6 h at room temperature. The solvent was removed in vacuo and the orange residue was purified by column chromatography (EtOAc as eluant) affording a yellow solid that was recrystallized from EtOAc/pentane to give desired compound **1** as a white solid (18 mg, 30% yield).

1H NMR (300 MHz, DMSO) δ 8.91 (s, 1H), 8.40 (dd, J = 8.7, 2.2, 2H), 8.17 (s, 1H), 8.16 (s, 1H), 8.01 (d, J = 8.5, 2H), 7.71 (m, 4H), 7.70 (d, J = 8.5, 2H), 7.30 (s, 1H), 5.71 (s, 2H), 1.68 (s, 6H).

Supplementary Methods

Kinase Assay

For the in vitro kinase assay flag-tagged ATM and ATR kinases were immunoprecipitated from 293T cells using Anti-flag M2 affinity gel (Sigma Aldrich A2220). As a substrate, p53/1-101 peptide fused to GST was purified from IPTG stimulated BL21 bacteria by conventional GST purification methods. Briefly, pCDNA3-flag-ATM and pBJF-flag-ATR plasmids (wild type and kinase dead versions) were transfected into 293T cells. 48 hours after transfection, cells were lysed in TGN buffer (50 mM Tris (pH 7.5), 50 mM glycerophosphate, 150 mM NaCl, 10% glycerol, 1% tween-20 and protease inhibitors cocktail) for 15 minutes on ice and, after centrifugation, the supernatant was pre-cleared for 1h with unspecific rabbit IgG and protein A on a rotator at 4 degrees. Next, the supernatant was incubated with M2-slurry for 2h at 4 degrees. For a confluent p100 plate of 293T cells, 400 µl of buffer, 10 µg of IgG, 30 µl of protein A slurry, and 25 µl of M2 beads were used. Anti flag M2 beads were then washed 5 times in ice cold TNG, 3 times in ice cold LiCl buffer (100mM Tris pH 7.5, 0.5 M LiCl), and 5 times in ice cold Kinase buffer (10 mM Hepes (pH 7.5), 50 mM NaCl, 10 mM MgCl2, 10 mM MnCl2, 1 mM DTT). After the last wash, IPs were splitted in the proper number of tubes for the assay (approximately one confluent 293T p100 was used per condition). For the kinase reaction, 100 µM 'cold' ATP was added to the buffer. Only fresh IPs were used. Prior to every experiment a mix was prepared containing 2 µg of GST-p53 and 10 µCi of ^{32}P-γATP per condition. ATRi or DDRi inhibitors were first added to the beads. Last, 25 µl of the mix were added to each tube. Reactions were performed for 20 minutes at 30 degrees and stopped by adding 15 microliters of 4x NuPAGE SDS buffer and boiling for 5 minutes. Beads were pelleted and supernatants were resolved by SDS-PAGE on a polyacrylamide gel. Radioactive gels were slightly washed and directly exposed to Phospor-Imager screens for 2h to 16h. Radioactivity was then detected using a STORM scanner. Finally, gels were stained with coomasie to check for protein levels. Flag-ATR and flag-ATM expression plasmids were kindly provided by K. Cimprich and M. Kastan labs respectively.

Supplementary References

1 Link, W. *et al.* Chemical interrogation of FOXO3a nuclear translocation identifies potent and selective inhibitors of phosphoinositide 3-kinases. *J Biol Chem* **284**, 28392-28400, (2009).

2 Beck, H. *et al.* Regulators of cyclin-dependent kinases are crucial for maintaining genome integrity in S phase. *J Cell Biol* **188**, 629-638, (2010) .

3 Murga, M. *et al.* A mouse model of ATR-Seckel shows embryonic DNA replicative stress and accelerated ageing. *Nat Genet* **41**,891-8, (2009).

4 Maira, S. M. *et al.* Identification and characterization of NVP-BEZ235, a new orally available dual phosphatidylinositol 3-kinase/mammalian target of rapamycin inhibitor with potent in vivo antitumor activity. *Mol Cancer Ther* **7**, 1851-1863, (2008).

5 Hickson, I. *et al.* Identification and characterization of a novel and specific inhibitor of the ataxia-telangiectasia mutated kinase ATM. *Cancer Res* **64**, 9152-9159, (2004).